Title
Accuracy and Precision of 3-dimensional Optical Imaging for Body Composition by Age, BMI, and Ethnicity.

Journal
The American Journal of Clinical Nutrition, 118(3)

Authors
Wong, Michael
Bennett, Jonathan
Quon, Brandon
et al.

Publication Date
2023-09-01

DOI
10.1016/j.ajcnut.2023.07.010

Peer reviewed

The American Journal of Clinical Nutrition 118 (2023) 657–671

The American Journal of
CLINICAL NUTRITION

journal homepage: https://ajcn.nutrition.org/

Original Research Article

Accuracy and Precision of 3-dimensional Optical Imaging for Body Composition by Age, BMI, and Ethnicity

Michael C. Wong [1,2], Jonathan P. Bennett [1,2], Brandon Quon [1], Lambert T. Leong [1], Isaac Y. Tian [3], Yong E. Liu [1], Nisa N. Kelly [1], Cassidy McCarthy [4], Dominic Chow [5], Sergi Pujades [6], Andrea K. Garber [7], Gertraud Maskarinec [1], Steven B. Heymsfield [4], John A. Shepherd [1,2,*]

[1] *Department of Epidemiology, University of Hawaii Cancer Center, Honolulu, HI, United States;* [2] *Department of Human Nutrition, Food and Animal Sciences, University of Hawaii at Manoa, Honolulu, HI, United States;* [3] *Paul G. Allen School of Computer Science and Engineering, University of Washington, Seattle, WA, United States;* [4] *Pennington Biomedical Research Center, Baton Rouge, LA, United States;* [5] *John A. Burns School of Medicine, University of Hawaii at Manoa, Honolulu, HI, United States;* [6] *Inria, Université Grenoble Alpes, CNRS, Grenoble INP, LJK, Grenoble, France;* [7] *Department of Pediatrics, University of California San Francisco, San Francisco, CA, United States*

A B S T R A C T

Background: The obesity epidemic brought a need for accessible methods to monitor body composition, as excess adiposity has been associated with cardiovascular disease, metabolic disorders, and some cancers. Recent 3-dimensional optical (3DO) imaging advancements have provided opportunities for assessing body composition. However, the accuracy and precision of an overall 3DO body composition model in specific subgroups are unknown.
Objectives: This study aimed to evaluate 3DO's accuracy and precision by subgroups of age, body mass index, and ethnicity.
Methods: A cross-sectional analysis was performed using data from the Shape Up! Adults study. Each participant received duplicate 3DO and dual-energy X-ray absorptiometry (DXA) scans. 3DO meshes were digitally registered and reposed using Meshcapade. Principal component analysis was performed on 3DO meshes. The resulting principal components estimated DXA whole-body and regional body composition using stepwise forward linear regression with 5-fold cross-validation. Duplicate 3DO and DXA scans were used for test–retest precision. Student's *t* tests were performed between 3DO and DXA by subgroup to determine significant differences.
Results: Six hundred thirty-four participants (females = 346) had completed the study at the time of the analysis. 3DO total fat mass in the entire sample achieved R^2 of 0.94 with root mean squared error (RMSE) of 2.91 kg compared to DXA in females and similarly in males. 3DO total fat mass achieved a % coefficient of variation (RMSE) of 1.76% (0.44 kg), whereas DXA was 0.98% (0.24 kg) in females and similarly in males. There were no mean differences for total fat, fat-free, percent fat, or visceral adipose tissue by age group ($P > 0.068$). However, there were mean differences for underweight, Asian, and Black females as well as Native Hawaiian or other Pacific Islanders ($P < 0.038$).
Conclusions: A single 3DO body composition model produced accurate and precise body composition estimates that can be used on diverse populations. However, adjustments to specific subgroups may be warranted to improve the accuracy in those that had significant differences.
This trial was registered at clinicaltrials.gov as NCT03637855 (Shape Up! Adults).

Keywords: body composition, three-dimensional optical, diversity, DXA, accuracy

Introduction

Obesity has been a growing epidemic for the past few generations and has led to the need for more accessible methods to monitor adiposity [1–3]. Excess adiposity is linked to the development of cardiovascular disease, type 2 diabetes, and up to 20% of cancers [4–6]. BMI is generally used to classify obesity. However, BMI only uses height and weight and does not account for muscle or FM, and therefore, it is a poor method for nutritional assessment on an individual level. Instead, body composition methods have been developed to quantify FM and FFM (lean soft tissue + bone masses) to characterize health status [7,8]. Furthermore, regional body composition such as visceral adipose tissue (VAT) has shown to be a better predictor than BMI for adverse outcomes such as type 2 diabetes (OR: 2.17 vs. 1.66)

Abbreviations: 3DO, 3-dimensional optical; LSC, least significant change; MD, mean difference; NHOPI, Native Hawaiian or Other Pacific Islander; PBRC, Pennington Biomedical Research Center; PC, principal component; UCSF, University of California, San Francisco; UHCC, University of Hawaii Cancer Center; VAT, visceral adipose tissue.

* Corresponding author
E-mail address: johnshep@hawaii.edu (J.A. Shepherd).

https://doi.org/10.1016/j.ajcnut.2023.07.010
Received 16 February 2023; Received in revised form 3 July 2023; Accepted 13 July 2023; Available online 19 July 2023

and hypertension (OR: 2.08 vs. 1.77) [9]. Studies have also shown ethnic differences when it comes to fat distribution such as higher levels of VAT in Japanese-Americans compared with their ethnic counterparts [10] as well as age-related differences [11].

Imaging methods such as MRI and CT are among criterion methods for regional body composition [12,13]. However, these methods are expensive; require trained/certified technicians; use ionizing radiation (CT), limiting frequent use; and have limited access outside clinical settings. DXA, air displacement plethysmography (ADP), and BIA are among the more accessible modalities developed for body composition, but they also have limitations including requiring trained technicians (DXA and ADP), ionizing radiation (DXA), physiological calibration assumptions (BIA), and lack of regional/compartmental compositions (ADP) [14–16]. The ideal method would include total and regional composition to be accurate in subgroups by sex, BMI, age, and ethnicity; free of ionizing radiation; self-operating; and low cost to operate.

In the last 2 decades, body shape defined in detail using 3-dimensional optical (3DO) imaging has been intensely explored as a health descriptor [17]. 3DO scanners generally output a detailed 3D mesh with over 100,000 sample points that represents the person's body shape and automated anthropometric estimates (ie, circumferences, lengths, surface areas, and volumes) [18–20]. From the early days until now, researchers validated the accuracy and precision of the automated anthropometry to criterion methods (eg, tape measurements to circumferences/lengths, underwater weighing or ADP to total volume) [20–22]. Researchers also showed that these automated anthropometric estimates, some of which would be difficult and tedious to obtain manually, were predictive of DXA FM and FFM [23–26].

Since 3DO anthropometry was as good if not better than manual measurements, as health descriptors, researchers attempted to create more advanced shape descriptors using the 3DO mesh to utilize the entire body. Since then, the methodology to obtain these body shape descriptors have improved by incorporating automated processing methods, pose-independent body composition models, a 2D image to 3D mesh pipeline, and agnostic body composition models across multiple 3DO scanners so that the models were no longer device specific [27–30].

Although much has been accomplished in this field in a short amount of time, body composition models created for 3DO scanners have not been interrogated for accuracy as a function of age, BMI, and ethnicity. Our hypothesis was that body shape is deterministically defined by the underlying distributions of fat and muscle, and when properly modeled, should accurately represent regional fat even when body shapes differ by sex, age, BMI, and ethnicity. The objective of this study was to evaluate the 3DO's total and regional body composition accuracy and precision in a diverse population stratified by sex, age, BMI, and ethnicity as compared to DXA.

Methods

Study design

Shape Up! Adults was a cross-sectional study of healthy adults (NIH R01 DK109008, clinicaltrials.gov NCT03637855). This study was designed to investigate the associations between body shape and composition with various health markers. Participants underwent a series of measures that included whole-body 3DO scans, DXA scans, blood serum tests, and functional strength tests.

Participants

Participants were recruited at Pennington Biomedical Research Center (PBRC), University of Hawaii Cancer Center (UHCC), and University of California, San Francisco (UCSF). All participants provided informed consent. The study protocol was approved by the Institutional Review Boards at PBRC (IRB study #2016-053), UCSF (IRB #15-18066), and the University of Hawaii Office of Research Compliance (CHS #2017-01018). Volunteers were prescreened over the phone and were deemed ineligible if they were pregnant, breastfeeding, had missing limbs, nonremovable metal, previous body-altering surgery (eg, breast augmentation, liposuction), hair that could not be contained in a swim cap, were unable to stand still for 1 min, or unable to lay still for 3 min.

Pretesting preparations included an 8-h fast (water and prescribed medications were allowed) and no strenuous exercise 24 h prior to the study visit. Participants were stratified by age (18–39, 40–59, ≥60 y), ethnicity (non-Hispanic White [White], non-Hispanic Black [Black], Hispanic, Asian, and Native Hawaiian or Other Pacific Islander [NHOPI]), sex, and BMI (<18.5 [underweight], 18.5–24.9 [normal weight], 25–29.9 [overweight], >30 [obese] kg/m^2) according to the World Health Organization [31]. Participants self-reported their ethnicity from the 5 ethnic subgroups. Height and weight were measured on a SECA 274 Stadiometer.

DXA

Participants received duplicate whole-body DXA scans with a Hologic Discovery/A or Horizon system according to International Society for Clinical Densitometry guidelines with repositioning [32]. Participants were scanned once, asked to get off the table, and laid back on the table for the second scan. The Hologic Whole-Body Phantom was scanned 10 times at each site with UCSF considered the gold standard site. Ratios between the gold standard site and the other sites were calculated. An ANOVA with a Dunnett test was applied to determine mean difference (MDs) between the sites and the gold standard site. There were no differences between UCSF and PBRC. There was a correction factor of 1.05036 between UCSF and UHCC for %fat. The Hologic Block Phantom was scanned daily for quality control to ensure the system did not fall out of calibration. No other corrections were needed. All scans were analyzed at UHCC by a single certified technologist using Hologic Apex version 5.6 with the NHANES Body Composition Analysis calibration option disabled [33]. Outputs included whole-body and regional FM and FFM measures.

3DO surface scans

Participants changed into form-fitting tights, a swim cap, and a sports bra if female. Duplicate 3DO surface scans were taken on the Fit3D ProScanner version 4.x within 10 min of each other and with repositioning. Participants grasped telescoping handles on the scanner platform and stood upright with shoulders relaxed and arms positioned straight and abducted from their torso. The platform rotates once around and takes approximately 45 s for the completion of the scan. Final point clouds were converted to a mesh connected by triangles with approximately 300,000 vertices and 600,000 faces to represent the body shape. Previous validation studies showed good agreement and precision for Fit3D's automated anthropometry in comparison to manual circumference measurements [19,22,24].

3DO meshes were registered and digitally reposed by Meshcapade. Their algorithm registers each mesh to a 110,000-vertex template with full anatomical correspondence. This means each vertex corresponds to a specific anatomical location across all registered meshes. Without the registration, the number of vertices and their locations would be random. Thus, the variance would not be comparable for analysis. Meshcapade's methods can be read in detail in Loper et al. [34]. All meshes were digitally reposed to a T-pose, where the person was standing straight, arms were brought horizontal and in plane with the body, and arms and legs were straightened. Previous work showed that reposing the mesh to a standardized position and pose reduced the precision error by approximately 50% [29].

Statistical shape modeling

Since vertices in the 3D meshes are highly correlated with neighboring vertices, principal component analysis was performed on the registered meshes to orthogonalize and reduce the dimensionality of the data so that fewer variables were needed to describe the data's variance while creating sex-specific statistical shape models [35]. The resulting outputs were principal components (PCs) that could be used for analysis.

Manifold regression images stratified by ethnicity and sex (Figures 1 and 2) were created by adjusting the PCs with the mean FM, FFM, and age, shown in Table 1 [3]. The adjusted PCs were then averaged and inverted back into coordinate space (x, y, and z) to obtain the image. The manifold images were a demonstration on how average body shape may differ by ethnicity when FM, FFM, and age are the same. With this visual example, regional MDs were added to show how different ethnic groups may hold FM and FFM from other ethnic counterparts. P values for the regional differences were also displayed on the images.

Mean images (Figures 3 and 4) stratified by sex, BMI, and ethnicity were created by averaging the PCs of the specific strata and inverting back into coordinate space to show a generalized average shape of that group. Groups with <1 participant did not have a mean image.

Statistical analysis

Stepwise forward linear regression with 5-fold cross-validation was used to predict DXA body composition with the PCs. The reported results were the average result of the 5 folds. The independent variables were the PCs and demographics (ie, age and BMI) (PC+DEMO model), whereas the dependent variables were DXA whole-body and

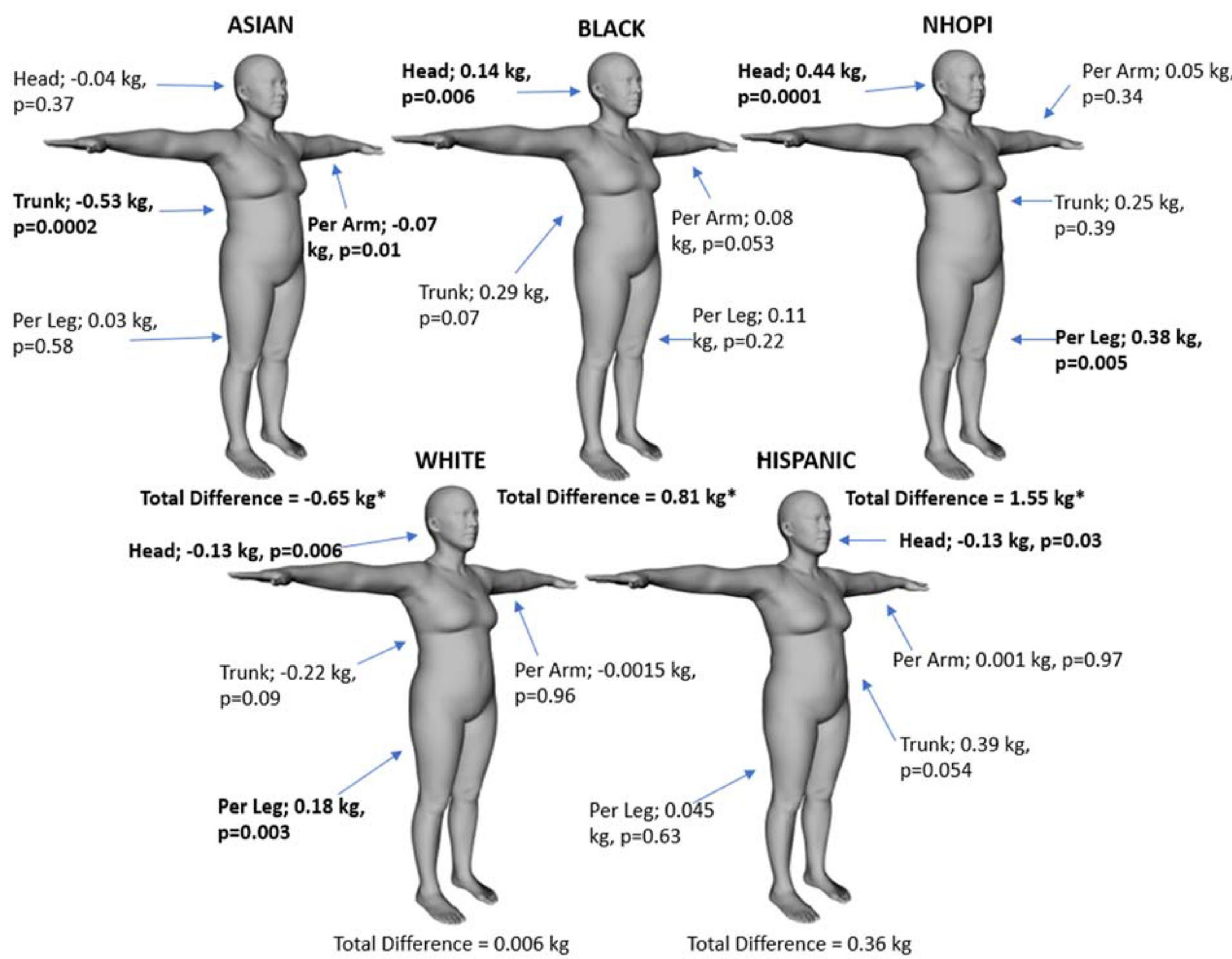

FIGURE 1. Female manifold regression images of different ethnic groups that were adjusted with the overall sample mean age and DXA total fat mass and fat-free mass (ie, 46.6 y, 25.4 kg, and 46.1 kg, respectively). This means each mesh, in theory, has the same age, fat, and fat-free masses. Regional differences (DXA – 3DO) are displayed to examine how different ethnic groups differ in body shape and composition even though they have the same total fat and fat-free masses. Bold print indicates a significant difference ($P < 0.05$) in total and regional fat masses between DXA and 3DO by Student's t test. 3DO, 3-dimensional optical; DXA, dual-energy X-ray absorptiometry.

regional body composition measures. PC-only models were created first and then adjusted with age and BMI as potential covariates for the PC + DEMO models. Only variables with a significance of $P < 0.5$ remained in each model. Results were reported with R^2 and RMSE. This model used the entire Shape Up! Adults cohort and was similar to previous models presented with an incomplete sample [28,29,35].

Test–retest precision, also known as short-term precision, was performed on the duplicate DXA and 3DO meshes. The %CV and RMSE were used to quantify the test–retest precision defined by Glüer et al. [36]. Subgroup precision was calculated using standard deviation between test–retest scans and averaged by group because RMSE between 2 scans could not be solved. Differences between subgroups were compared within the strata of age, BMI, and ethnicity with a 1-factor ANOVA. A P value < 0.05 was considered statistically significant.

The accuracy of 3DO total FM, FFM, and %fat was evaluated at the subgroup level with the stratifications mentioned previously. MDs were calculated between 3DO estimates from the PC + DEMO model and DXA (3DO – DXA). Paired Student's t test determined if the differences were statistically significant ($P < 0.05$). If significant, the %MD would be calculated [(DXA – 3DO) / DXA × 100]. Percent MDs under 2% were considered small, 2% to 5% moderate, and >5% large. All analyses were performed in R version 4.2.1 (R Core Teams).

Results

At the time of this analysis, 883 participants were available. Two hundred forty-nine participants were excluded for different study protocol ($n = 181$), dropouts ($n = 7$), missing or unusable 3DO scan ($n = 48$), or invalid DXA scan ($n = 13$) (Supplemental Figure 1). After exclusions, 634 participants remained in the analysis (Table 1). In total, 225, 302, and 108 participants were recruited from UCSF, PBRC, and UHCC, respectively. The female and male ethnic distributions were similar to NHANES for White and Black participants. However, the Shape Up! Adults recruitment had about 10% more Asian and 10% less Hispanic participants compared with NHANES [37].

The first 3 PC modes captured 95% of the shape variance in each of the female and male shape models. 3DO PC-only equations were highly correlated to DXA body composition values (Table 2). 3DO total FM and FFM in females achieved R^2s of 0.94 and 0.92 with

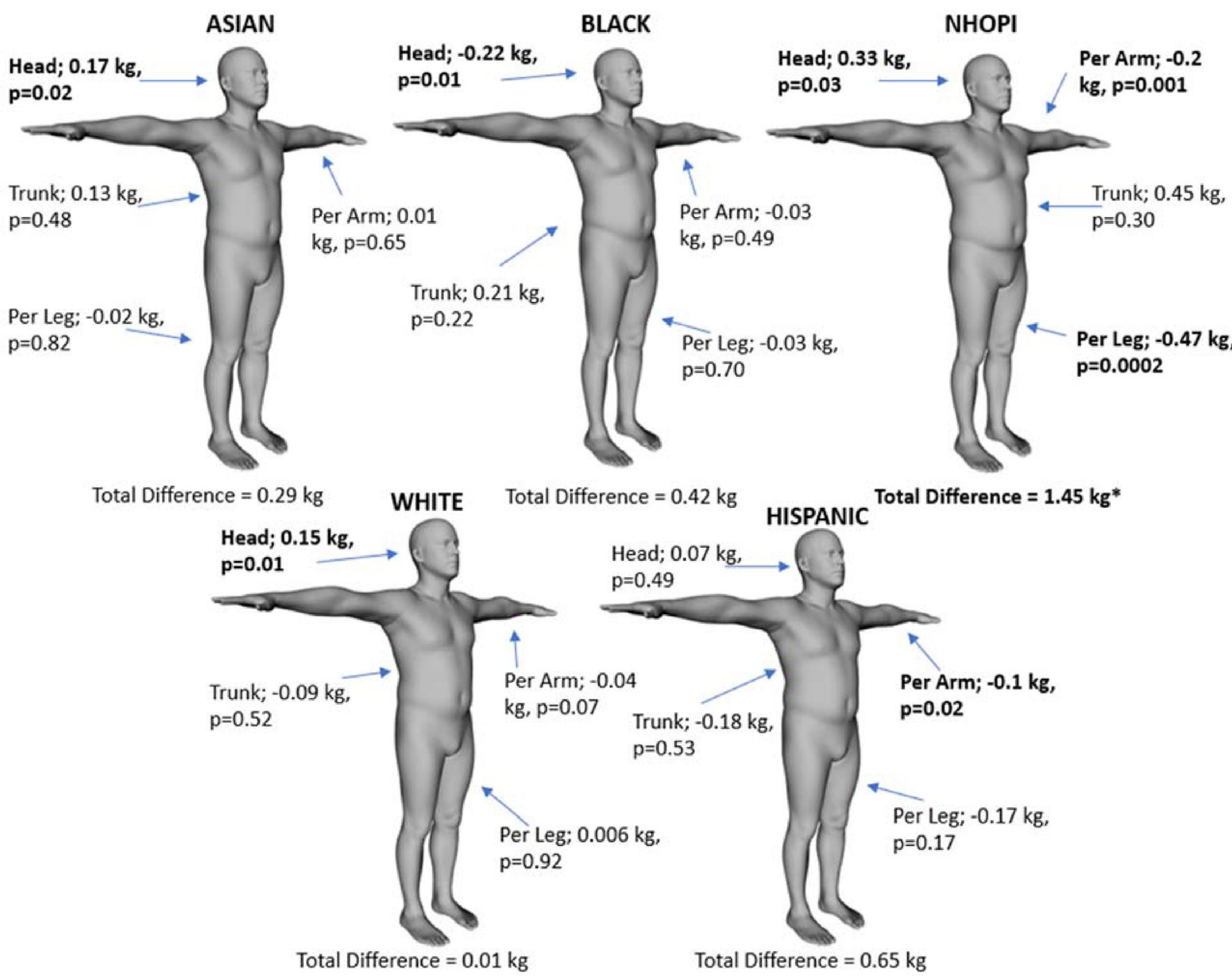

FIGURE 2. Male manifold regression images of different ethnic groups that were adjusted with the overall sample mean age and DXA total fat mass and fat-free mass (ie, 43.5 y, 20.9 kg, and 66.6 kg, respectively). This means each mesh, in theory, has the same age, fat, and fat-free masses. Regional differences (DXA – 3DO) are displayed to examine how different ethnic groups differ in body shape and composition even though they have the same total fat and fat-free masses. Bold print indicates a significant difference ($P < 0.05$) in total and regional fat masses between DXA and 3DO by Student's t test. 3DO, 3-dimensional optical; DXA, dual-energy X-ray absorptiometry.

TABLE 1
Sample characteristics by age group and BMI category

	Female															
	Ages 18–39 y				Ages 40–59 y				Ages ≥60 y				Overall			
	Underweight	**Normal**	**Overweight**	**Obese**	**Underweight**	**Normal**	**Overweight**	**Obese**	**Underweight**	**Normal**	**Overweight**	**Obese**	**Underweight**	**Normal**	**Overweight**	**Obese**
	(*N* = 9)	**(*N* = 44)**	**(*N* = 38)**	**(*N* = 38)**	**(*N* = 10)**	**(*N* = 43)**	**(*N* = 33)**	**(*N* = 36)**	**(*N* = 6)**	**(*N* = 39)**	**(*N* = 26)**	**(*N* = 24)**	**(*N* = 25)**	**(*N* = 126)**	**(*N* = 97)**	**(*N* = 98)**
Age (y)																
Mean (SD)	24.3 (5.98)	28.0 (5.93)	29.3 (5.75)	31.1 (5.77)	52.5 (4.55)	49.6 (5.57)	52.1 (5.81)	48.3 (5.61)	66.3 (2.73)	66.4 (5.33)	66.4 (3.79)	64.6 (3.34)	45.7 (17.8)	47.2 (16.7)	47.0 (16.2)	45.6 (14.2)
[Min, Max]	[18.0, 35.0]	[18.0, 39.0]	[19.0, 39.0]	[18.0, 39.0]	[42.0, 56.0]	[41.0, 59.0]	[40.0, 59.0]	[40.0, 59.0]	[62.0, 70.0]	[60.0, 89.0]	[60.0, 75.0]	[60.0, 71.0]	[18.0, 70.0]	[18.0, 89.0]	[19.0, 75.0]	[18.0, 71.0]
Ethnicity																
Asian	3 (33.3%)	8 (18.2%)	10 (26.3%)	6 (15.8%)	5 (50.0%)	14 (32.6%)	6 (18.2%)	7 (19.4%)	1 (16.7%)	14 (35.9%)	6 (23.1%)	2 (8.3%)	9 (36.0%)	36 (28.6%)	22 (22.7%)	15 (15.3%)
Black	0 (0%)	9 (20.5%)	6 (15.8%)	11 (28.9%)	1 (10.0%)	7 (16.3%)	9 (27.3%)	6 (16.7%)	1 (16.7%)	7 (17.9%)	6 (23.1%)	9 (37.5%)	2 (8.0%)	23 (18.3%)	21 (21.6%)	26 (26.5%)
Hispanic	1 (11.1%)	12 (27.3%)	4 (10.5%)	6 (15.8%)	0 (0%)	7 (16.3%)	6 (18.2%)	5 (13.9%)	0 (0%)	3 (7.7%)	2 (7.7%)	2 (8.3%)	1 (4.0%)	22 (17.5%)	12 (12.4%)	13 (13.3%)
NHOPI	0 (0%)	3 (6.8%)	6 (15.8%)	7 (18.4%)	0 (0%)	4 (9.3%)	3 (9.1%)	4 (11.1%)	0 (0%)	1 (2.6%)	0 (0%)	1 (4.2%)	0 (0%)	8 (6.3%)	9 (9.3%)	12 (12.2%)
White	5 (55.6%)	12 (27.3%)	12 (31.6%)	8 (21.1%)	4 (40.0%)	11 (25.6%)	9 (27.3%)	14 (38.9%)	4 (66.7%)	14 (35.9%)	12 (46.2%)	10 (41.7%)	13 (52.0%)	37 (29.4%)	33 (34.0%)	32 (32.7%)
Height (cm)																
Mean (SD)	163 (7.98)	164 (6.29)	163 (7.98)	162 (6.76)	163 (7.09)	164 (6.86)	163 (5.14)	163 (6.21)	164 (5.13)	160 (7.45)	160 (8.29)	161 (5.57)	163 (6.76)	163 (7.05)	162 (7.32)	162 (6.27)
[Min, Max]	[151, 176]	[151, 180]	[149, 181]	[146, 174]	[155, 177]	[150, 181]	[154, 171]	[147, 176]	[157, 173]	[144, 178]	[149, 190]	[151, 171]	[151, 177]	[144, 181]	[149, 190]	[146, 176]
Weight (kg)																
Mean (SD)	45.3 (5.94)	58.3 (5.93)	72.5 (7.31)	98.4 (20.3)	45.6 (4.95)	59.2 (7.71)	73.2 (5.91)	98.1 (19.6)	47.3 (4.20)	54.8 (5.81)	70.2 (9.02)	87.2 (7.91)	45.9 (5.03)	57.5 (6.76)	72.1 (7.41)	95.5 (18.3)
[Min, Max]	[38.6, 55.4]	[44.5, 72.5]	[60.9, 88.8]	[70.5, 153]	[35.4, 53.0]	[44.2, 75.2]	[61.0, 85.0]	[66.3, 146]	[42.2, 52.3]	[41.7, 67.6]	[60.0, 103]	[73.6, 102]	[35.4, 55.4]	[41.7, 75.2]	[60.0, 103]	[66.3, 153]
BMI (kg/m^2)																
Mean (SD)	17.0 (1.11)	21.7 (1.81)	27.1 (1.18)	37.5 (6.73)	17.1 (1.26)	21.9 (1.88)	27.5 (1.22)	36.8 (6.51)	17.6 (0.905)	21.4 (1.92)	27.4 (1.33)	33.6 (3.11)	17.2 (1.11)	21.7 (1.86)	27.3 (1.24)	36.3 (6.11)
[Min, Max]	[14.8, 18.4]	[18.6, 24.8]	[25.1, 29.6]	[30.0, 51.9]	[14.2, 18.4]	[18.7, 24.9]	[25.2, 29.9]	[30.1, 53.1]	[16.0, 18.4]	[18.6, 24.4]	[25.1, 29.6]	[30.0, 40.9]	[14.2, 18.4]	[18.6, 24.9]	[25.1, 29.9]	[30.0, 53.1]
Total FM (kg)																
Mean (SD)	10.7 (2.81)	16.4 (3.93)	24.3 (4.12)	39.7 (13.1)	9.49 (2.08)	17.5 (4.21)	27.5 (3.64)	40.3 (9.91)	10.9 (1.74)	17.0 (3.89)	26.6 (4.16)	36.7 (6.64)	10.3 (2.31)	17.0 (4.01)	26.0 (4.18)	39.2 (10.6)
[Min, Max]	[7.20, 14.6]	[8.31, 27.4]	[11.9, 32.7]	[22.7, 72.7]	[6.30, 12.2]	[9.31, 27.2]	[18.6, 35.0]	[27.9, 67.8]	[9.08, 13.1]	[10.4, 25.5]	[16.4, 34.7]	[22.4, 48.9]	[6.30, 14.6]	[8.31, 27.4]	[11.9, 35.0]	[22.4, 72.7]
Total FFM (kg)																
Mean (SD)	34.4 (3.64)	42.0 (4.55)	47.9 (5.37)	58.6 (9.14)	36.1 (4.71)	41.6 (5.45)	45.7 (4.32)	56.6 (9.88)	36.1 (3.42)	37.9 (4.51)	43.2 (8.26)	50.4 (4.00)	35.5 (3.98)	40.6 (5.17)	45.9 (6.15)	55.9 (9.02)
[Min, Max]	[30.0, 41.6]	[28.9, 52.5]	[39.8, 61.3]	[42.1, 80.4]	[28.6, 43.6]	[30.9, 53.8]	[37.1, 53.2]	[37.1, 77.5]	[32.2, 40.9]	[29.0, 47.5]	[33.7, 75.6]	[42.4, 58.0]	[28.6, 43.6]	[28.9, 53.8]	[33.7, 75.6]	[37.1, 80.4]
Percent body fat (%)																
Mean (SD)	23.5 (3.91)	27.9 (5.19)	33.6 (4.43)	39.6 (5.89)	20.9 (4.23)	29.5 (5.03)	37.5 (3.66)	41.4 (3.37)	23.3 (2.93)	30.9 (5.61)	38.3 (5.48)	41.9 (4.76)	22.4 (3.90)	29.4 (5.36)	36.2 (4.90)	40.8 (4.88)
[Min, Max]	[18.8, 29.6]	[15.2, 37.6]	[17.2, 39.2]	[28.7, 53.3]	[12.6, 27.1]	[18.7, 39.3]	[30.3, 45.2]	[34.9, 48.3]	[18.2, 26.6]	[20.4, 44.8]	[26.6, 45.6]	[30.5, 48.6]	[12.6, 29.6]	[15.2, 44.8]	[17.2, 45.6]	[28.7, 53.3]
VAT (kg)																
Mean (SD)	0.11 (0.03)	0.17 (0.07)	0.30 (0.10)	0.57 (0.31)	0.11 (0.03)	0.29 (0.14)	0.56 (0.20)	0.82 (0.28)	0.13 (0.07)	0.36 (0.18)	0.65 (0.19)	0.80 (0.23)	0.11 (0.04)	0.27 (0.16)	0.48 (0.22)	0.72 (0.30)
[Min, Max]	[0.05, 0.15]	[0.07, 0.34]	[0.11, 0.51]	[0.09, 1.37]	[0.06, 0.17]	[0.08, 0.61]	[0.24, 1.14]	[0.31, 1.32]	[0.07, 0.23]	[0.08, 0.90]	[0.30, 1.14]	[0.49, 1.22]	[0.05, 0.23]	[0.07, 0.90]	[0.11, 1.14]	[0.09, 1.37]
	Males **(*N* = 2)**	**(*N* = 37)**	**(*N* = 59)**	**(*N* = 34)**	**(*N* = 1)**	**(*N* = 82)**	**(*N* = 32)**	**(*N* = 38)**	**(*N* = 1)**	**(*N* = 22)**	**(*N* = 22)**	**(*N* = 17)**	**(*N* = 4)**	**(*N* = 82)**	**(*N* = 113)**	**(*N* = 89)**
Age (y)																
Mean (SD)	29.0 (5.66)	26.6 (5.47)	29.6 (6.11)	30.4 (5.84)	48.0 (NA)	43.8 (18.1)	48.9 (5.78)	49.6 (6.20)	67.0 (NA)	67.6 (5.71)	65.9 (4.78)	63.6 (3.20)	43.3 (18.5)	43.8 (18.1)	42.1 (15.5)	45.0 (13.7)
[Min, Max]	29.0 [25.0, 33.0]	25.0 [18.0, 37.0]	30.0 [19.0, 39.0]	32.0 [18.0, 39.0]	48.0 [48.0, 48.0]	42.0 [18.0, 79.0]	48.5 [40.0, 59.0]	50.0 [40.0, 59.0]	67.0 [67.0, 67.0]	66.0 [60.0, 79.0]	64.5 [60.0, 77.0]	62.0 [60.0, 71.0]	40.5 [25.0, 67.0]	42.0 [18.0, 79.0]	38.0 [19.0, 77.0]	44.0 [18.0, 71.0]
Ethnicity																
Asian	2 (100%)	9 (24.3%)	18 (30.5%)	7 (20.6%)	0 (0%)		9 (28.1%)	8 (21.1%)	0 (0%)	7 (31.8%)	5 (22.7%)	2 (11.8%)	2 (50.0%)		32 (28.3%)	

(*continued on next page*)

TABLE 1 (*continued*)

	Female															
	Ages 18–39 y				Ages 40–59 y				Ages ≥60 y				Overall			
	Underweight	**Normal**	**Overweight**	**Obese**	**Underweight**	**Normal**	**Overweight**	**Obese**	**Underweight**	**Normal**	**Overweight**	**Obese**	**Underweight**	**Normal**	**Overweight**	**Obese**
	(*N* = 9)	**(*N* = 44)**	**(*N* = 38)**	**(*N* = 38)**	**(*N* = 10)**	**(*N* = 43)**	**(*N* = 33)**	**(*N* = 36)**	**(*N* = 6)**	**(*N* = 39)**	**(*N* = 26)**	**(*N* = 24)**	**(*N* = 25)**	**(*N* = 126)**	**(*N* = 97)**	**(*N* = 98)**
						22 (26.8%)								22 (26.8%)		17 (19.1%)
Black	0 (0%)	8 (21.6%)	8 (13.6%)	9 (26.5%)	1 (100%)	16 (19.5%)	7 (21.9%)	8 (21.1%)	1 (100%)	3 (13.6%)	8 (36.4%)	6 (35.3%)	2 (50.0%)	16 (19.5%)	23 (20.4%)	23 (25.8%)
Hispanic	0 (0%)	8 (21.6%)	9 (15.3%)	5 (14.7%)	0 (0%)	12 (14.6%)	2 (6.3%)	3 (7.9%)	0 (0%)	1 (4.5%)	1 (4.5%)	1 (5.9%)	0 (0%)	12 (14.6%)	12 (10.6%)	9 (10.1%)
NHOPI	0 (0%)	2 (5.4%)	6 (10.2%)	4 (11.8%)	0 (0%)	2 (2.4%)	1 (3.1%)	4 (10.5%)	0 (0%)	0 (0%)	0 (0%)	0 (0%)	0 (0%)	2 (2.4%)	7 (6.2%)	8 (9.0%)
White	0 (0%)	10 (27.0%)	18 (30.5%)	9 (26.5%)	0 (0%)	30 (36.6%)	13 (40.6%)	15 (39.5%)	0 (0%)	11 (50.0%)	8 (36.4%)	8 (47.1%)	0 (0%)	30 (36.6%)	39 (34.5%)	32 (36.0%)
Height (cm)																
Mean (SD)	164 (12.7)	176 (7.61)	176 (7.02)	176 (9.37)	175 (NA)	176 (7.45)	174 (6.07)	177 (7.18)	151 (NA)	175 (7.21)	175 (7.35)	176 (7.66)	163 (12.1)	176 (7.45)	175 (6.79)	177 (8.10)
[Min, Max]	[155, 173]	[162, 190]	[159, 192]	[147, 202]	[175, 175]	[159, 192]	[163, 188]	[161, 190]	[151, 151]	[159, 188]	[155, 188]	[158, 187]	[151, 175]	[159, 192]	[155, 192]	[147, 202]
Weight (kg)																
Mean (SD)	47.1 (9.23)	67.9 (8.28)	85.1 (8.95)	110 (17.2)	56.1 (NA)	69.2 (8.22)	82.5 (7.21)	110 (17.4)	41.5 (NA)	68.0 (7.57)	83.2 (8.46)	113 (15.4)	48.0 (8.04)	69.2 (8.22)	84.0 (8.41)	110 (16.8)
[Min, Max]	[40.6, 53.7]	[51.4, 81.2]	[63.9, 104]	[70.6, 149]	[56.1, 56.1]	[51.4, 90.2]	[69.1, 97.6]	[88.4, 174]	[41.5, 41.5]	[54.1, 82.4]	[62.1, 100]	[79.4, 149]	[40.6, 56.1]	[51.4, 90.2]	[62.1, 104]	[70.6, 174]
Weight (kg/m^2)																
Mean (SD)	17.5 (0.735)	21.9 (1.79)	27.5 (1.50)	35.4 (4.76)	18.4 (NA)	22.3 (1.78)	27.1 (1.43)	34.8 (4.38)	18.2 (NA)	22.2 (1.82)	27.2 (1.30)	36.3 (4.37)	17.9 (0.627)	22.3 (1.78)	27.3 (1.44)	35.3 (4.51)
[Min, Max]	[17.0, 18.0]	[18.7, 25.0]	[25.0, 30.0]	[30.1, 49.2]	[18.4, 18.4]	[18.6, 25.0]	[25.0, 29.5]	[30.1, 52.6]	[18.2, 18.2]	[18.6, 24.6]	[25.0, 29.9]	[30.3, 47.3]	[17.0, 18.4]	[18.6, 25.0]	[25.0, 30.0]	[30.1, 52.6]
Total FM (kg)																
Mean (SD)	8.93 (2.98)	11.0 (3.39)	18.7 (5.50)	29.9 (10.6)	8.30 (NA)	12.6 (4.21)	19.1 (4.04)	31.7 (9.03)	5.01 (NA)	14.4 (4.16)	20.1 (3.56)	34.3 (8.70)	7.79 (2.55)	12.6 (4.21)	19.1 (4.78)	31.6 (9.58)
[Min, Max]	[6.82, 11.0]	[5.13, 20.0]	[9.05, 29.4]	[11.9, 45.9]	[8.30, 8.30]	[5.13, 26.5]	[7.44, 27.3]	[20.5, 66.5]	[5.01, 5.01]	[7.33, 21.5]	[14.3, 26.7]	[20.5, 48.9]	[5.01, 11.0]	[5.13, 26.5]	[7.44, 29.4]	[11.9, 66.5]
Total FFM (kg)																
Mean (SD)	38.4 (6.28)	57.2 (7.35)	66.7 (7.76)	81.0 (9.72)	48.0 (NA)	56.9 (7.17)	63.5 (6.59)	77.9 (10.9)	35.7 (NA)	54.3 (6.11)	62.9 (7.15)	78.4 (9.41)	40.1 (6.51)	56.9 (7.17)	65.1 (7.46)	79.1 (10.2)
[Min, Max]	[33.9, 42.8]	[43.7, 73.0]	[47.2, 86.0]	[65.1, 108]	[48.0, 48.0]	[40.6, 73.0]	[50.4, 78.2]	[62.6, 106]	[35.7, 35.7]	[40.6, 67.8]	[46.4, 74.2]	[58.6, 99.4]	[33.9, 48.0]	[40.6, 73.0]	[46.4, 86.0]	[58.6, 108]
Percent body fat (%)																
Mean (SD)	18.6 (2.65)	16.0 (4.26)	21.8 (5.57)	26.4 (7.16)	14.7 (NA)	18.0 (5.08)	23.1 (4.53)	28.7 (4.63)	12.3 (NA)	20.7 (4.58)	24.3 (3.57)	30.1 (4.97)	16.1 (3.47)	18.0 (5.08)	22.6 (5.02)	28.2 (5.84)
[Min, Max]	[16.7, 20.5]	[9.91, 25.1]	[10.6, 32.8]	[13.6, 38.6]	[14.7, 14.7]	[9.03, 32.6]	[10.2, 31.5]	[20.3, 38.6]	[12.3, 12.3]	[11.5, 31.6]	[16.6, 31.6]	[20.7, 38.4]	[12.3, 20.5]	[9.03, 32.6]	[10.2, 32.8]	[13.6, 38.6]
VAT (kg)																
Mean (SD)	0.20 (0.01)	0.23 (0.047)	0.33 (0.09)	0.52 (0.22)	0.22 (NA)	0.32 (0.16)	0.49 (0.16)	0.79 (0.32)	0.16 (NA)	0.46 (0.18)	0.69 (0.24)	0.91 (0.29)	0.20 (0.03)	0.32 (0.16)	0.45 (0.20)	0.72 (0.32)
[Min, Max]	[0.20, 0.21]	[0.16, 0.33]	[0.18, 0.63]	[0.22, 1.04]	[0.22, 0.22]	[0.16, 0.91]	[0.17, 0.73]	[0.29, 1.64]	[0.16, 0.16]	[0.20, 0.91]	[0.29, 1.22]	[0.35, 1.31]	[0.16, 0.22]	[0.16, 0.91]	[0.17, 1.22]	[0.22, 1.64]

Abbreviations: NA, not applicable; NHOPI, Native Hawaiian and other Pacific Islanders; SD, standard deviation; VAT, visceral adipose tissue.
Body composition values measured from dual-energy X-ray absorptiometry.

RMSEs of 2.91 kg and 2.76 kg, whereas males achieved R^2s of 0.94 and 0.94 with RMSEs of 3.04 kg and 2.97 kg, respectively. Female and male 3DO %fat had moderate correlations with DXA (R^2: 0.75 and 0.73; RMSE: 3.82% and 3.31%, respectively). Regional 3DO FM and FFM estimates (ie, arms, legs, and trunk) had moderate to strong correlations with DXA (R^2 range: 0.79–0.95, RMSE range: 0.27–1.86 kg) for females and males. After possible adjustments for age and BMI as covariates (PC + DEMO), there were marginal improvements to the R^2s and RMSEs.

3DO test–retest precision was comparable to DXA (Table 3). 3DO total FM and FFM achieved a %CV (RMSE) of 1.76% (0.44 kg) and 0.96% (0.44 kg) in females, whereas DXA had a %CV (RMSE) of 0.98% (0.24 kg) and 0.59% (0.27 kg), respectively. In females, 3DO VAT, arm FM, and trunk FM (%CV: 4.4%, 2.72%, and 1.55%; RMSE: 0.02 kg, 0.04 kg, and 0.18 kg, respectively) achieved better test–retest precision than DXA (%CV: 8.08%, 3.16%, and 2.04%; RMSE: 0.03 kg, 0.05 kg, and 0.23 kg, respectively). Test–retest precision in males showed similar results. However, only 3DO VAT had better test–retest

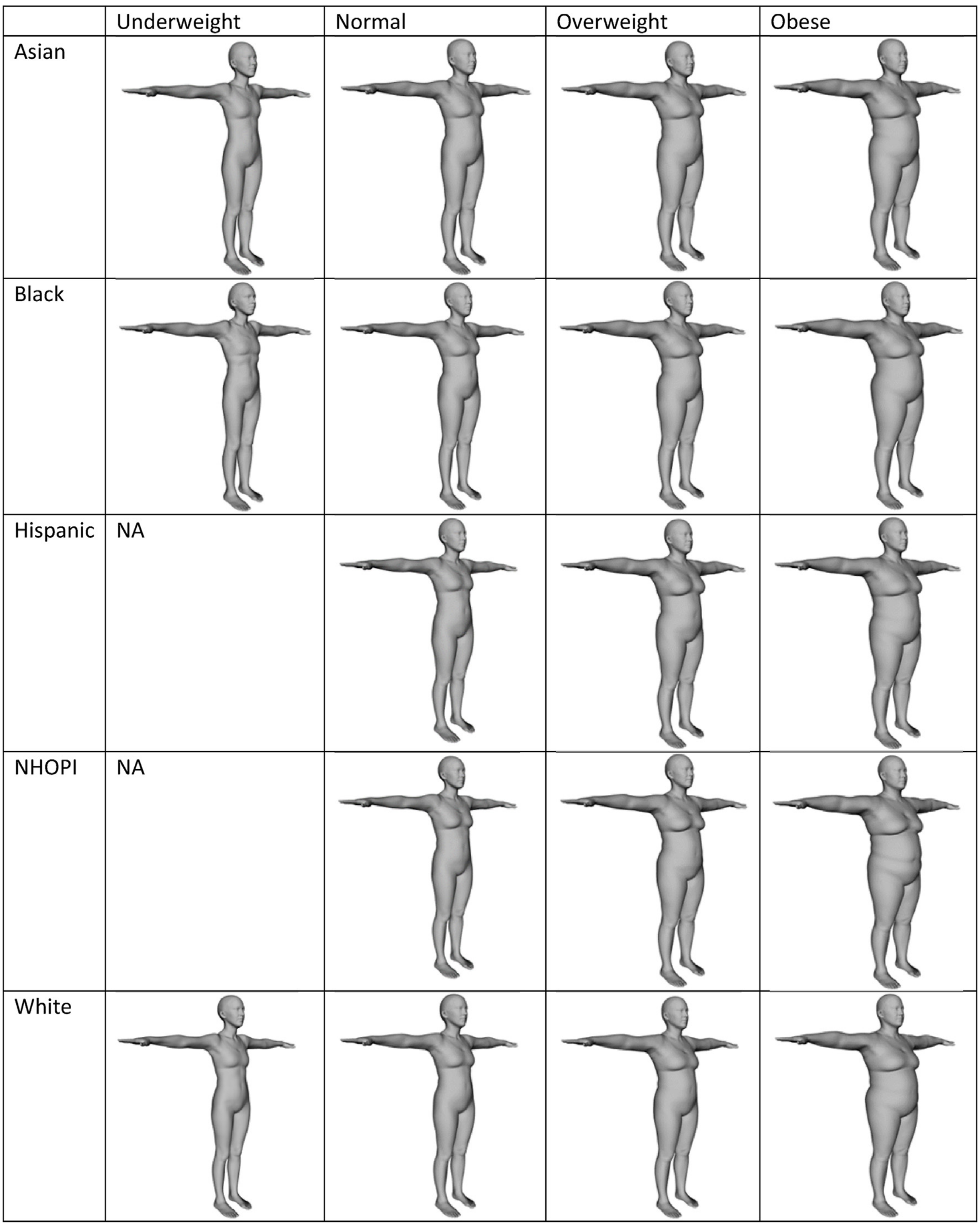

FIGURE 3. Female mean body shape images stratified by BMI and ethnicity. NA indicates that there was ≤ 1 participant, so a mean image could not be derived. BMI, body mass index.

precision than DXA in males. When comparing the precision across subgroups of age, BMI, and ethnicity with 1-factor ANOVA, there were no significant differences for all 3DO whole-body and regional body composition outputs (data not shown, $P > 0.06$).

When comparing 3DO total FM, FFM, %fat, and VAT to DXA by age subgroups (Table 4), there were no MDs in either females or males ($P > 0.068$). For the BMI subgroups (Table 5), females with underweight had significant differences for total FM, FFM, and %fat (MDs: 1.23 kg, −1.23 kg, and 3.12%, respectively, $P < 0.014$) as well as %fat for the females with obesity (MD = −0.79%, $P = 0.023$). There were no MDs across the male BMI subgroups ($P > 0.314$). In the ethnicity subgroups (Table 6), female Asian, Black, and NHOPI subgroups had MDs in total FM (MDs: 0.64 kg, −0.81 kg, −1.55 kg%, respectively), FFM (MDs: −1.6 kg, 1.7 kg, and 3 kg%, respectively), and %fat (MDs: 1.38%, −1.11%, and −2.24%, respectively) ($P < 0.017$). Additionally, the male NHOPI subgroup had MDs for total FM, FFM, and %fat (MDs: −1.45 kg, 1.45 kg, and −1.88%, respectively; $P < 0.038$). If ethnicity was added to the model (data not shown), differences in ethnicity subgroups were no longer significant ($P > 0.99$). However, underweight females still had a MD ($P = 0.029$).

Average shape images were created for both males and females by ethnic group (Figures 1 and 2) to show MDs by region. Asians had significant differences in the trunk and arm measures, Blacks had differences in the head measures, and NHOPIs had differences in the head and leg measures. Although difficult to see in the figures, Black females on average had longer legs and shorter torsos, whereas NHOPI

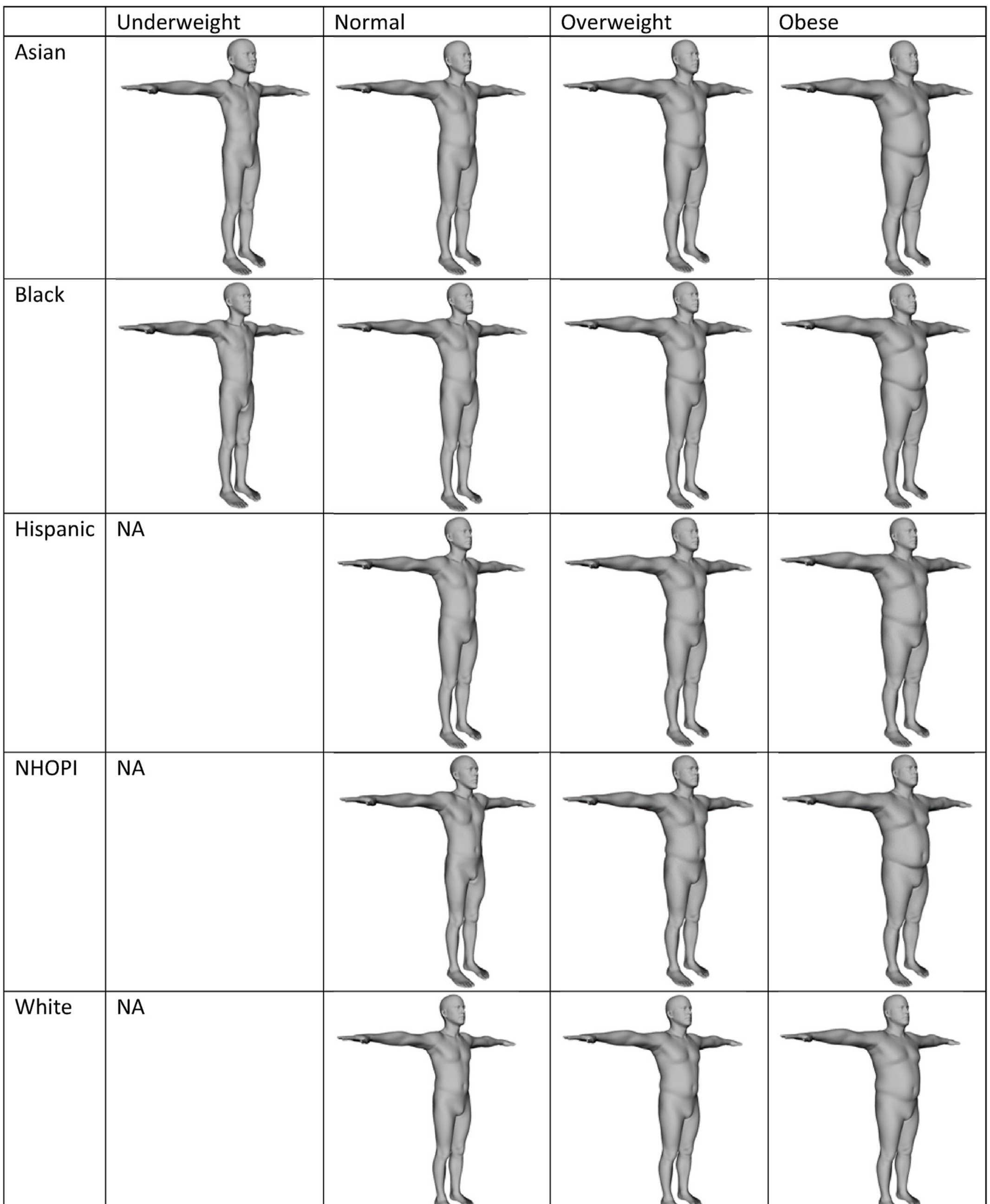

FIGURE 4. Male mean body shape images stratified by BMI and ethnicity. NA indicates that there was ≤ 1 participant, so a mean image could not be derived. BMI, body mass index.

TABLE 2

3D optical body composition models from stepwise forward linear regression to estimate to DXA body composition (mean results from 5-fold cross-validation)

Sex	Outcome	PC-only				PC + Demographics			
		Variable	Coefficient	R^2	RMSE	Variable	Coefficient	R^2	RMSE
Females	Total FM	Intercept	26.5689	0.94	2.91	Intercept	16.4494	0.94	2.88
		PC1	0.1282			PC1	0.1108		
		PC2	2.0930			PC2	1.5903		
		PC3	-1.0575			PC3	-0.7970		
		PC4	0.7487			PC4	0.5483		
		PC5	0.5329			PC5	0.4035		
		PC6	-0.4188			PC6	-0.2978		
		PC7	-1.3200			PC7	-0.9192		
		PC9	-0.4824			PC9	-0.7256		
		PC10	1.6580			PC10	1.1085		
		PC11	1.8068			PC11	1.4661		
		PC13	-2.7090			PC13	-2.3351		
						BMI	0.3597		
	Total FFM	Total Mass - Total Fat Mass		0.92	2.76	Total Mass - Total Fat Mass		0.92	2.63
	Percent Fat	Total Fat Mass / Total Mass		0.75	3.82	Total Fat Mass / Total Mass		0.75	3.76
	VAT	Intercept	0.4516	0.72	0.15	Intercept	0.3334	0.78	0.14
		PC2	0.0408			PC2	0.0431		
		PC3	-0.0226			PC3	-0.0254		
		PC4	0.0151			PC4	0.0142		
		PC5	-0.0332			PC5	-0.0252		
		PC6	0.0554			PC6	0.0417		
		PC7	0.0349			PC7	0.0382		
		PC8	-0.0680			PC8	-0.0931		
		PC12	-0.0809			PC12	-0.0301		
		PC13	-0.0348			PC13	-0.0569		
		PC14	-0.0489			PC14	-0.0555		
		PC15	-0.0570			PC15	-0.0490		
						Age	0.0028		
	Arm FM	Intercept	1.6889	0.86	0.34	Intercept	0.6964	0.87	0.33
		PC1	0.0073			PC1	0.0058		
		PC2	0.1508			PC2	0.1023		
		PC3	-0.0723			PC3	-0.0508		
		PC4	0.0354			PC4	0.0242		
		PC7	-0.0391			PC7	-0.0176		
		PC8	-0.0928			PC8	-0.0755		
		PC10	0.0857			PC10	0.0553		
		PC11	0.1248			PC11	0.0901		
		PC13	-0.0635			PC13	-0.0259		
		PC14	0.1282			PC14	0.0937		
						BMI	0.0356		
	Arm FFM	Intercept	2.4555	0.81	0.27	Intercept	1.7392	0.81	0.27
		PC1	0.0159			PC1	0.0141		
		PC2	0.0791			PC2	0.0423		
		PC4	-0.0283			PC4	-0.0308		
		PC5	0.0653			PC5	0.0427		
		PC6	-0.0587			PC6	-0.0469		
		PC7	0.0945			PC7	0.0748		
		PC8	-0.0871			PC8	-0.0601		
		PC9	0.0919			PC9	0.0999		
		PC11	-0.0678			PC11	-0.0745		
		PC12	0.1752			PC12	0.1223		
		PC13	0.1557			PC13	0.1900		
		PC14	0.1555			PC14	0.1657		
						BMI	0.0253		
	Leg FM	Intercept	4.9806	0.89	0.77	Intercept	-0.7249	0.9	0.7
		PC1	0.0301			PC1	0.0225		
		PC2	0.3257			PC2	0.0640		
		PC3	-0.1496			PC3	-0.0395		
		PC4	0.1742			PC4	0.0844		
		PC5	0.2336			PC5	0.1576		
		PC6	-0.3811			PC6	-0.3458		
		PC7	-0.6359			PC7	-0.5000		
		PC8	0.2286			PC8	0.3740		
		PC9	-0.1582			PC9	-0.1925		
		PC10	0.6106			PC10	0.3756		
		PC11	0.4500			PC11	0.2694		
		PC13	-0.6444			PC13	-0.4967		
						Age	0.0090		
						BMI	0.1886		
	Leg FFM	Intercept	7.6220	0.86	0.69	Intercept	2.1961	0.88	0.61
		PC1	0.0535			PC1	0.0432		
		PC2	0.2321			PC2	-0.0418		
		PC3	-0.0540			PC3	0.0506		
		PC4	-0.0477			PC4	-0.0836		
		PC5	0.2668			PC5	0.1021		
		PC6	-0.2926			PC6	-0.1679		
		PC12	0.5220			PC12	0.2473		
		PC13	0.2352			PC13	0.3576		
		PC14	0.4598			PC14	0.3194		
						Age	-0.0064		
						BMI	0.2051		
	Trunk FM	Intercept	12.2398	0.95	1.45	Intercept	12.2398	0.95	1.45
		PC1	0.0523			PC1	0.0523		

(continued on next page)

TABLE 2 (*continued*)

Sex	Outcome	PC-only				PC + Demographics			
		Variable	Coefficient	R^2	RMSE	Variable	Coefficient	R^2	RMSE
		PC2	1.1211			PC2	1.1211		
		PC3	-0.6125			PC3	-0.6125		
		PC4	0.3434			PC4	0.3434		
		PC6	0.3615			PC6	0.3615		
		PC8	-0.7211			PC8	-0.7211		
		PC10	0.3308			PC10	0.3308		
		PC11	0.6288			PC11	0.6288		
		PC13	-1.3325			PC13	-1.3325		
		PC15	-0.5152			PC15	-0.5152		
	Trunk FFM	Intercept	23.3186	0.9	1.55	Intercept	15.7269	0.9	1.56
		PC1	0.1303			PC1	0.1205		
		PC2	0.7044			PC2	0.3419		
		PC3	-0.3264			PC3	-0.1800		
		PC4	-0.2970			PC4	-0.3386		
		PC5	0.3798			PC5	0.2091		
		PC6	0.1300			PC6	0.2489		
		PC7	0.6023			PC7	0.6429		
		PC8	-0.5750			PC8	-0.3958		
		PC11	0.4349			PC11	0.1498		
		PC12	0.7638			PC12	0.5748		
		PC13	0.2979			PC13	0.4630		
		PC14	0.7890			PC14	0.6475		
		PC15	0.5148			PC15	0.4326		
						BMI	0.2745		
Males	Total FM	Intercept	23.4226	0.94	3.04	Intercept	24.2945	0.94	2.85
		PC1	-0.1924			PC1	-0.1883		
		PC2	2.0747			PC2	1.9407		
		PC3	-1.4689			PC3	-1.3345		
		PC4	-1.2207			PC4	-1.2314		
		PC5	0.9020			PC5	0.9058		
		PC6	0.6394			PC6	0.5996		
		PC7	-2.3710			PC7	-1.8262		
		PC8	0.9488			PC8	0.8188		
		PC9	-1.5091			PC9	-1.6708		
		PC10	-1.4176			PC10	-0.6422		
		PC11	2.8085			PC11	2.6083		
		PC12	2.0674			PC12	1.5622		
		PC14	1.1338			PC14	1.1794		
		PC15	-1.2783			PC15	-1.1086		
						Age	-0.0311		
	Total FFM	Total Mass - Total Fat Mass		0.94	2.97	Total Mass - Total Fat Mass		0.95	2.63
	Percent Fat	Total Fat Mass / Total Mass		0.73	3.31	Total Fat Mass / Total Mass		0.77	3.17
	VAT	Intercept	0.5050	0.73	0.14	Intercept	0.3881	0.75	0.14
		PC1	-0.0025			PC1	-0.0024		
		PC2	0.0360			PC2	0.0382		
		PC3	-0.0256			PC3	-0.0280		
		PC4	-0.0489			PC4	-0.0390		
		PC5	0.0712			PC5	0.0616		
		PC6	0.0489			PC6	0.0401		
		PC7	0.0919			PC7	0.0633		
		PC9	-0.0505			PC9	-0.0340		
		PC10	0.0453			PC10	0.0206		
		PC11	0.0859			PC11	0.0641		
		PC13	-0.0786			PC13	-0.0813		
		PC14	0.0598			PC14	0.0437		
		PC15	0.0984			PC15	0.0930		
						Age	0.0030		
	Arm FM	Intercept	1.4169	0.86	0.3	Intercept	1.4169	0.86	0.3
		PC1	-0.0109			PC1	-0.0109		
		PC2	0.1403			PC2	0.1403		
		PC3	-0.0888			PC3	-0.0888		
		PC4	-0.0633			PC4	-0.0633		
		PC5	0.0538			PC5	0.0538		
		PC7	-0.1132			PC7	-0.1132		
		PC8	0.0640			PC8	0.0640		
		PC11	0.1479			PC11	0.1478		
		PC12	0.1454			PC12	0.1454		
		PC15	-0.0818			PC15	-0.0818		
	Arm FFM	Intercept	4.3909	0.79	0.43	Intercept	-2.2843	0.88	0.36
		PC1	-0.0246			PC1	-0.0089		
		PC2	0.1095			PC2	-0.1596		
		PC3	0.0468			PC3	0.1405		
		PC4	0.0861			PC4	0.2015		
		PC5	-0.2594			PC5	-0.1733		
		PC6	-0.1831			PC6	-0.1072		
		PC7	0.2161			PC7	0.1650		
		PC8	-0.1722			PC8	-0.2115		
		PC9	0.2050			PC9	0.3574		
		PC11	-0.3739			PC11	-0.4795		
		PC12	0.1182			PC12	-0.0916		
		PC14	-0.2356			PC14	-0.1463		
		PC15	0.1522			PC15	0.1853		
						Age	0.0070		
						BMI	0.2198		

(*continued on next page*)

TABLE 2 (*continued*)

Sex	Outcome	PC-only				PC + Demographics			
		Variable	Coefficient	R^2	RMSE	Variable	Coefficient	R^2	RMSE
	Leg FM	Intercept	3.8794	0.88	0.7	Intercept	3.8794	0.88	0.7
		PC1	-0.0329			PC1	-0.0329		
		PC2	0.3032			PC2	0.3032		
		PC3	-0.2220			PC3	-0.2221		
		PC4	-0.1629			PC4	-0.1629		
		PC7	-0.8775			PC7	-0.8775		
		PC8	0.1725			PC8	0.1725		
		PC9	-0.3007			PC9	-0.3007		
		PC10	-0.4316			PC10	-0.4316		
		PC11	0.4213			PC11	0.4213		
		PC12	0.4360			PC12	0.4360		
		PC15	-0.6294			PC15	-0.6294		
	Leg FFM	Intercept	11.0904	0.84	0.84	Intercept	6.5031	0.85	0.81
		PC1	-0.0678			PC1	-0.0537		
		PC2	0.2644			PC2	0.0743		
		PC4	0.0760			PC4	0.1364		
		PC5	-0.4727			PC5	-0.4295		
		PC6	-0.4029			PC6	-0.3450		
		PC11	-0.2748			PC11	-0.2650		
		PC12	0.4749			PC12	0.3277		
		PC14	-0.3186			PC14	-0.2001		
						BMI	0.1572		
	Trunk FM	Intercept	11.6548	0.94	1.66	Intercept	12.2359	0.94	1.54
		PC1	-0.1024			PC1	-0.1009		
		PC2	1.1661			PC2	1.1352		
		PC3	-0.8335			PC3	-0.8090		
		PC4	-0.7817			PC4	-0.7977		
		PC5	0.8185			PC5	0.8424		
		PC6	0.5521			PC6	0.5651		
		PC7	-0.3729			PC7	-0.2483		
		PC8	0.4690			PC8	0.3791		
		PC9	-0.8747			PC9	-0.9111		
		PC10	-0.5862			PC10	-0.4334		
		PC11	1.6527			PC11	1.5991		
		PC12	0.9004			PC12	0.7377		
		PC14	0.8207			PC14	0.7938		
						Age	-0.0152		
	Trunk FFM	Intercept	32.6704	0.91	1.86	Intercept	18.9138	0.91	1.83
		PC1	-0.1891			PC1	-0.1519		
		PC2	0.9060			PC2	0.3550		
		PC3	-0.2653			PC3	-0.0705		
		PC4	0.3630			PC4	0.5238		
		PC5	-0.5713			PC5	-0.3227		
		PC6	-0.7049			PC6	-0.4851		
		PC7	1.2259			PC7	1.1442		
		PC11	-0.6362			PC11	-0.6084		
		PC12	0.8325			PC12	0.1553		
		PC14	-0.6104			PC14	-0.4821		
						BMI	0.4737		

Abbreviations: DXA, dual-energy X-ray absorptiometry; PC, principal component; RMSE, root mean squared error; VAT, visceral adipose tissue.
PC-only: stepwise forward linear regression with only PCs as possible predictors of DXA body composition outputs.
PC+Demographics: stepwise forward linear regression with PCs, age, and BMI as possible predictors of DXA body composition outputs.

females held more mass in the torso, compared with their Asian counterparts. White males were taller on average, whereas NHOPIs held more mass in their abdomen on average, compared with other ethnicities.

Discussion

In this study, 3DO body composition accuracy and precision were evaluated at the subgroup level of age, BMI, and ethnicity. Accuracy of subgroups was compared to DXA, whereas precision was an intragroup comparison. The analysis showed MDs in accuracy among females with underweight, NHOPI females and males, and Asian and Black females, whereas all other groups showed no differences. We detected no significant differences in precision among the subgroups. Differences between 3DO and DXA body composition measures were not observed in 19 out of the 24 subgroups that were evaluated. However, it is worth noting that 3 of the 5 subgroups where differences were observed were among female ethnicity subgroups. However, it is important to keep in mind the differences with small to moderate % MD. Specific equations may be needed for those groups with differences.

Overall, the accuracy and precision were similar to previous work done by our group on interim analysis of the cohort that used the Fit3D [29]. The previous publication reported total FM R^2s of 0.90 and 0.95

TABLE 3
Test–retest precision of 3D optical and DXA in %CV (RMSE) (n = 639)

Variable	DXA Female	3DO Female	DXA Male	3DO Male
Total FM, kg	0.98 (0.24)	1.76 (0.44)	1.37 (0.28)	2.93 (0.60)
Total FFM, kg	0.59 (0.27)	0.96 (0.44)	0.55 (0.36)	0.91 (0.60)
Percent Fat, %	NA (0.33)	NA (0.66)	NA (0.31)	NA (0.74)
VAT, kg	8.08 (0.03)	4.40 (0.02)	6.88 (0.03)	4.78 (0.02)
Arm FM, kg	3.16 (0.05)	2.72 (0.04)	3.43 (0.04)	3.99 (0.05)
Arm FFM, kg	2.14 (0.05)	2.57 (0.06)	1.89 (0.08)	1.94 (0.08)
Leg FM, kg	1.47 (0.07)	2.90 (0.14)	2.34 (0.08)	4.29 (0.14)
Leg FFM, kg	1.13 (0.08)	1.95 (0.14)	1.18 (0.13)	1.22 (0.13)
Trunk FM, kg	2.04 (0.23)	1.55 (0.18)	2.42 (0.25)	3.03 (0.31)
Trunk FFM, kg	1.16 (0.26)	1.52 (0.34)	1.07 (0.34)	1.20 (0.38)

Abbreviations: 3DO, 3-dimensional optical; CV, coefficient of variation; DXA, dual-energy X-ray absorptiometry; RMSE, root mean squared error; VAT, visceral adipose tissue.

TABLE 4
3D optical vs. DXA body composition by age group

Sex	Groups	*n*	Variable	Mean Difference	% Mean Difference	*P*
Female	Young	126	Total FM	-0.28	N.S.	0.303
	Middle Aged	119	Total FM	0.05	N.S.	0.828
	Senior	89	Total FM	-0.03	N.S.	0.901
	Young	126	Total FFM	0.28	N.S.	0.303
	Middle Aged	119	Total FFM	-0.05	N.S.	0.828
	Senior	89	Total FFM	0.03	N.S.	0.901
	Young	126	%Fat	-0.23	N.S.	0.559
	Middle Aged	119	%Fat	0.19	N.S.	0.566
	Senior	89	%Fat	0.04	N.S.	0.932
	Young	126	VAT	-0.01	N.S.	0.204
	Middle Aged	119	VAT	0.02	N.S.	0.068
	Senior	89	VAT	-0.01	N.S.	0.438
Male	Young	127	Total FM	-0.01	N.S.	0.960
	Middle Aged	93	Total FM	0.25	N.S.	0.373
	Senior	61	Total FM	-0.36	N.S.	0.288
	Young	127	Total FFM	0.01	N.S.	0.960
	Middle Aged	93	Total FFM	-0.25	N.S.	0.373
	Senior	61	Total FFM	0.36	N.S.	0.288
	Young	127	%Fat	0.03	N.S.	0.923
	Middle Aged	93	%Fat	0.35	N.S.	0.261
	Senior	61	%Fat	-0.37	N.S.	0.384
	Young	127	VAT	-0.00	N.S.	0.893
	Middle Aged	93	VAT	0.01	N.S.	0.508
	Senior	61	VAT	-0.01	N.S.	0.589

Abbreviations: 3DO, 3-dimensional optical; DXA, dual-energy X-ray absorptiometry; %Fat, percent fat; N.S., not significant; VAT, visceral adipose tissue.
Mean differences = 3DO – DXA; *P* value: Student's *t* test between 3DO and DXA
PC+Demo model was used in this comparison. FM, FFM, and VAT are measured in kg.
Young (18–39 y old), middle aged (40–59 y old), senior (≥60 y old).

for males (n = 159) and females (n = 202), respectively, which was similar to the current analysis. The follow-up analysis used 3 different 3DO scanners to build an agnostic model and reported total FM R^2s of 0.93 and 0.94 for males and females, respectively [28]. However, we had not previously presented subgroup analysis due to the limited statistical power.

In the female underweight group, there was a large difference between 3DO and DXA for total FM and a moderate difference for FFM (%MD = 12% and −3.4%, respectively). The %MD was proportionately higher despite a small difference due to the lower FM in the underweight group (approximately 10 kg). Another factor could be ethnicity because models were not initially adjusted for this. Female

TABLE 5
3D optical vs. DXA body composition by BMI

Sex	Groups	*n*	Variable	Mean Difference	%Mean Difference	*P*
Female	Underweight	24	Total FM	**1.23**	**12**	0.014*
	Normal	119	Total FM	-0.01	N.S.	0.958
	Overweight	94	Total FM	-0.13	N.S.	0.610
	Obese	96	Total FM	-0.54	N.S.	0.099
	Underweight	24	Total FFM	**-1.23**	**-3.4**	0.014*
	Normal	89	Total FFM	0.01	N.S.	0.958
	Overweight	94	Total FFM	0.13	N.S.	0.610
	Obese	96	Total FFM	0.54	N.S.	0.099
	Underweight	24	%Fat	**3.12**	—	0.010*
	Normal	119	%Fat	-0.10	N.S.	0.785
	Overweight	94	%Fat	-0.18	N.S.	0.616
	Obese	96	%Fat	**-0.79**	—	0.023*
	Underweight	24	VAT	-0.01	N.S.	0.772
	Normal	119	VAT	-0.01	N.S.	0.238
	Overweight	94	VAT	0.01	N.S.	0.286
	Obese	96	VAT	0.00	N.S.	0.988
Male	Underweight	3	Total FM	2.97	N.S.	0.155
	Normal	80	Total FM	0.11	N.S.	0.701
	Overweight	112	Total FM	-0.06	N.S.	0.779
	Obese	85	Total FM	-0.16	N.S.	0.633
	Underweight	3	Total FFM	-2.97	N.S.	0.155
	Normal	80	Total FFM	-0.11	N.S.	0.701
	Overweight	112	Total FFM	0.06	N.S.	0.779
	Obese	85	Total FFM	0.16	N.S.	0.633
	Underweight	3	%Fat	7.12	N.S.	0.168
	Normal	80	%Fat	0.21	N.S.	0.601
	Overweight	112	%Fat	-0.06	N.S.	0.804
	Obese	85	%Fat	-0.29	N.S.	0.356
	Underweight	3	VAT	-0.04	N.S.	0.407
	Normal	80	VAT	-0.01	N.S.	0.347
	Overweight	112	VAT	0.01	N.S.	0.380
	Obese	85	VAT	0.00	N.S.	0.936

Abbreviations: 3DO, 3-dimensional optical; BMI, body mass index; DXA, dual-energy X-ray absorptiometry; %Fat, percent fat; N.S., not significant; VAT, visceral adipose tissue.
Mean differences = 3DO - DXA; *P* value: Student's *t* test between 3DO and DXA
PC+Demo model was used in this comparison. FM, FFM, and VAT are measured in kg.
BMI classifications: Underweight (BMI <18.5), Normal (18.5–24.9), Overweight (25–29.9), Obese (BMI ≥ 30)
* p-values less than 0.05.

TABLE 6
3D optical vs. DXA body composition by ethnic group

Sex	Groups	n	Variable	Mean Difference	%Mean Difference	P-Value
Female	Asian	80	Total FM	**0.64**	**3.5**	0.017*
	Black	70	Total FM	**-0.81**	**-2.6**	0.015*
	Hispanic	47	Total FM	0.36	N.S.	0.386
	NHOPI	28	Total FM	**-1.55**	**-5.4**	0.003*
	White	107	Total FM	0.01	N.S.	0.980
	Asian	80	Total FFM	**-0.64**	**-1.6**	0.017*
	Black	70	Total FFM	**0.81**	**1.7**	0.015*
	Hispanic	47	Total FFM	-0.36	N.S.	0.386
	NHOPI	28	Total FFM	**1.55**	**3**	0.003*
	White	107	Total FFM	-0.01	N.S.	0.980
	Asian	80	%Fat	**1.38**	—	0.006*
	Black	70	%Fat	**-1.11**	—	0.010*
	Hispanic	47	%Fat	0.63	N.S.	0.305
	NHOPI	28	%Fat	**-2.24**	—	0.002*
	White	107	%Fat	-0.01	N.S.	0.979
	Asian	80	VAT	-0.00	N.S.	0.908
	Black	70	VAT	-0.02	N.S.	0.189
	Hispanic	47	VAT	0.01	N.S.	0.627
	NHOPI	28	VAT	-0.00	N.S.	0.942
	White	107	VAT	0.01	N.S.	0.362
Male	Asian	71	Total FM	0.29	N.S.	0.360
	Black	62	Total FM	0.42	N.S.	0.164
	Hispanic	32	Total FM	-0.65	N.S.	0.226
	NHOPI	16	Total FM	**-1.45**	**-6.5**	0.038*
	White	98	Total FM	-0.01	N.S.	0.958
	Asian	71	Total FFM	-0.29	N.S.	0.360
	Black	62	Total FFM	-0.42	N.S.	0.164
	Hispanic	32	Total FFM	0.65	N.S.	0.226
	NHOPI	16	Total FFM	**1.45**	**1.9**	0.038*
	White	98	Total FFM	0.01	N.S.	0.958
	Asian	71	%Fat	0.50	N.S.	0.258
	Black	62	%Fat	0.57	N.S.	0.093
	Hispanic	32	%Fat	-0.57	N.S.	0.374
	NHOPI	16	%Fat	**-1.88**	—	0.013*
	White	98	%Fat	-0.08	N.S.	0.789
	Asian	71	VAT	-0.01	N.S.	0.421
	Black	62	VAT	-0.03	N.S.	0.105
	Hispanic	32	VAT	0.02	N.S.	0.159
	NHOPI	16	VAT	0.02	N.S.	0.669
	White	98	VAT	0.02	N.S.	0.159

Abbreviations: 3DO, 3-dimensional optical; DXA, dual-energy X-ray absorptiometry; %Fat, percent fat; NHOPI, Native Hawaiian or other Pacific Islander; N.S., not significant; VAT, visceral adipose tissue.
Mean differences = 3DO - DXA; *P* value: Student's *t* test between 3DO and DXA
PC+Demo model was used in this comparison. FM, FFM, and VAT are measured in kg.
* p-values less than 0.05.

Asians, Blacks, and NHOPIs had MDs, and 44% of the underweight group were either Asian or Black. However, after adjustment for ethnicity, 3DO still overestimated total FM in underweight females. Thus, our models may not have seen enough shape variance in the underweight sample (underrepresentation) or other unique shape features from this group. The female subgroup with obesity also had a MD in %fat (−0.79%). However, this MD was very small, especially in a group with the highest mean %fat (41%). Since the difference was small and the total FM and FFM were not significant, the %fat difference may have been due to chance. It is worth noting that females with obesity may exhibit greater shape variability due to differences in how fat is distributed throughout their bodies. Specifically, the location of fat deposition may vary among the abdomen, hips, or appendages [38]. The largest differences were seen in the NHOPI group for both males and females. The differences may be driven by the low representation in comparison to other ethnic groups. In addition, differences in shape can also be driving these differences. Certain shape characteristics in Asian, Black, and NHOPI participants could be different from the majority of the group, which led to under- or overestimations as shown in Figure 1.

Compared with other studies that reported the accuracy by subgroups, Graybeal et al. [39] examined the accuracy of 3DO body composition estimates derived from smartphone-based applications (apps) with respect to the 4C model. For the HALO app, the authors reported a MD for total FM in males (MD: 2.1 kg; $P < 0.001$) but not in females (MD: 0.2 kg). In addition, they reported MDs for total FM in Whites and Blacks (MD: 0.9 kg and 1.0 kg, respectively; $P < 0.05$). In comparison to the current study, we did not observe MDs by sex or in the White ethnic group. However, we also reported MDs in the Black, female ethnic group. It is worth pointing out that our criterion was DXA, whereas Graybeal et al. used the 4C model.

Although not related to the Fit3D, other investigators have explored novel methods of using 2D imaging for body composition from accessible smartphone technology. The 2D methods generally capture an image(s) of a person and utilize machine learning methods to estimate body composition values to criterion methods such as DXA or the 4C model. Our previous study used 2D images taken from consumer-grade cameras and used the silhouettes to create a 3D mesh, which was used to estimate the body composition. We reported total FM R^2s of 0.96 and 0.94 in male and female test sets, respectively [30]. Nana et al. [40] reported 3DO body composition accuracy by sex from another smartphone app, Body Composition Technologies, with respects to DXA. The authors reported a %fat MD of 0.1% and −0.1% for males and females, respectively, which was similar to our findings. Farina et al. [41] developed a method to estimate DXA body composition using demographics and lateral surface image occupancy. The authors achieved R^2s of 0.97 and 0.95 for females and males, respectively, which was marginally better than ours. However, our sample size was about 5.4 times larger. Aside from traditional, commercial 3DO scanners, 2D methods showed promising results. Further investigation is warranted to evaluate the 2D methods' ability to monitor changes and accuracy across different ethnic, age, and BMI subgroups.

Other groups have also examined the precision of 3DO devices. Tinsley et al. [42] evaluated the precision the Fit3D ProScanner, Styku S100, Naked, and Size Stream SS20. Although the precision reported was not broken into subgroups, the overall precision of the devices achieved a %CV that ranged from 2.5% to 4.3% for total FM and 0.7% to 1.4% for total FFM with the Fit3D ProScanner at the high end for FM and FFM. Compared to the results in Table 3, our modeling method achieved a lower %CV with a larger sample size. Additionally, we did not observe differences in precision by subgroups using our models. The precision of the device/model will determine the ability to monitor smaller changes [43]. Additional evaluation of subgroup precision is necessary to validate the monitoring of FM and FFM changes in specific subgroups using commercial body composition systems.

The strength of the study was the scrutiny at the subgroup level. Although other studies have looked at accuracy by sex, BMI, and ethnicity, the current analysis examined more strata. In addition, only a single equation was needed for the majority of the subgroups that were explored. A subgroup-specific equation may be needed for those with MDs. However, there were also limitations. Some subgroups were underrepresented (ie, NHOPI and underweight). As such, the outcomes and interpretations of these groups should be cautioned as they were not as powered. The current analysis was completed with a healthy sample, so the results may not be applicable to patients with body composition-altering diseases. Future work can focus on populations with diseases that need constant body composition monitoring (younger populations [birth to 17 y]), and more accessible 3DO methods such as apps from smartphones [44,45].

In conclusion, 3DO body composition has advanced greatly in accuracy and precision in recent years. This work provides further insight of 3DO's ability to estimate body composition. Although 19 of the 24 subgroups had MDs from DXA, the majority of the subgroups did not display MDs using a single 3DO body composition model. Specific equations for the 5 subgroups that had MDs may improve the agreement. Beyond clinical settings, the accessibility and safety of these devices are appealing for those that want to monitor body composition frequently.

Acknowledgments

We thank all the participants for graciously giving their time to be part of the studies, our collaborators at each site for their part in the study, Tyler Carter and Greg Moore at Fit3D for providing us the 3DO data, and Naureen Mahmood and Talha Zaman for providing us the application program interface to register and repose our 3DO data.

Author contributions

The authors' responsibilities were as follows – MCW, JAS: designed and conducted the research; MCW, BQ, JAS: were part of the data analysis; MCW, YEL, NNK, CM, AKG, GM, SBH, JAS: were in charge of their respective study recruitment and protocols; MCW, JAS: drafted the manuscript and were responsible over the final content; and all authors: read and approved the final manuscript.

Conflict of interest

SBH reports his role on the Medical Advisory Boards of Tanita Corporation, Amgen, and Medifast; he is also an Amazon Scholar. JAS reports his role as a scientific advisor for Styku and Hologic. All other authors report no conflicts of interest.

Funding

Phases of this study were funded by the National Institute of Diabetes and Digestive and Kidney Diseases (NIH R01DK109008).

Data availability

Data described in the manuscript, code book, and analytic code will be made available upon request pending researchers who meet the criteria for access to confidential data. To request an application or to use our statistical shape model to transform your Meshcapade processed mesh into usable principal components, please contact John Shepherd (johnshep@hawaii.edu) or visit www.shapeup.shepherdresearchlab.org.

Appendix A. Supplementary data

Supplementary data to this article can be found online at https://doi.org/10.1016/j.ajcnut.2023.07.010.

References

[1] J. Bennett, M.C. Wong, C. McCarthy, N. Fearnbach, K. Queen, J. Shepherd, et al., Emergence of the adolescent obesity epidemic in the United States: five-decade visualization with humanoid avatars, Int. J. Obes. (Lond) 46 (9) (2022) 1587–1590, https://doi.org/10.1038/s41366-022-01153-9.

[2] C.M. Hales, M.D. Carroll, C.D. Fryar, C.L. Ogden, Prevalence of obesity and severe obesity among adults: United States, 2017-2018 [Internet], 2020. Available from: https://www.cdc.gov/nchs/products/databriefs/db360.htm.

[3] M.C. Wong, C. McCarthy, N. Fearnbach, S. Yang, J. Shepherd, S.B. Heymsfield, Emergence of the obesity epidemic: 6-decade visualization with humanoid avatars, Am. J. Clin. Nutr. 115 (4) (2022) 1189–1193, https://doi.org/10.1093/ajcn/nqac005.

[4] E.E. Calle, C. Rodriguez, K. Walker-Thurmond, M.J. Thun, Overweight, obesity, and mortality from cancer in a prospectively studied cohort of U.S. adults, N. Engl. J. Med. 348 (17) (2003) 1625–1638, https://doi.org/10.1056/NEJMoa021423.

[5] J.P. Després, I. Lemieux, Abdominal obesity and metabolic syndrome, Nature 444 (7121) (2006) 881–887, https://doi.org/10.1038/nature05488.

[6] S.M. Grundy, Obesity, metabolic syndrome, and cardiovascular disease, J. Clin. Endocrinol. Metab. 89 (6) (2004) 2595–2600, https://doi.org/10.1210/jc.2004-0372.

[7] M.J. Müller, M. Lagerpusch, J. Enderle, B. Schautz, M. Heller, A. Bosy-Westphal, Beyond the body mass index: tracking body composition in the pathogenesis of obesity and the metabolic syndrome, Obes. Rev. 13 (13) (2012) 6–13, https://doi.org/10.1111/j.1467-789X.2012.01033.x, suppl 2.

[8] L.C. Ward, Human body composition: yesterday, today, and tomorrow, Eur. J. Clin. Nutr. 72 (9) (2018) 1201–1207, https://doi.org/10.1038/s41430-018-0210-2.

[9] K. Direk, M. Cecelja, W. Astle, P. Chowienczyk, T.D. Spector, M. Falchi, et al., The relationship between DXA-based and anthropometric measures of visceral fat and morbidity in women, BMC Cardiovasc. Disord. 13 (1) (2013) 25, https://doi.org/10.1186/1471-2261-13-25.

[10] U. Lim, K.R. Monroe, S. Buchthal, B. Fan, I. Cheng, B.S. Kristal, et al., Propensity for intra-abdominal and hepatic adiposity varies among ethnic groups, Gastroenterology 156 (4) (2019) 966–975.e10, https://doi.org/10.1053/j.gastro.2018.11.021.

[11] G. Maskarinec, Y.B. Shvetsov, M.C. Wong, A. Garber, K. Monroe, T.M. Ernst, et al., Subcutaneous and visceral fat assessment by DXA and MRI in older adults and children, Obesity (Silver Spring) 30 (4) (2022) 920–930, https://doi.org/10.1002/oby.23381.

[12] S.B. Heymsfield, Z. Wang, R.N. Baumgartner, R. Ross, Human body composition: advances in models and methods, Annu. Rev. Nutr. 17 (1) (1997) 527–558, https://doi.org/10.1146/annurev.nutr.17.1.527.

[13] H.C. Lukaski, Methods for the assessment of human body composition: traditional and new, Am. J. Clin. Nutr. 46 (4) (1987) 537–556, https://doi.org/10.1093/ajcn/46.4.537.

[14] J.A. Shepherd, B.K. Ng, M.J. Sommer, S.B. Heymsfield, Body composition by DXA, Bone 104 (2017) 101–105, https://doi.org/10.1016/j.bone.2017.06.010.

[15] M.A. McCrory, T.D. Gomez, E.M. Bernauer, P.A. Molé, Evaluation of a new air displacement plethysmograph for measuring human body composition, Med. Sci. Sports Exerc. 27 (12) (1995) 1686–1691, https://doi.org/10.1249/00005768-199512000-00016.

[16] M. Abu Khaled, M.J. McCutcheon, S. Reddy, P.L. Pearman, G.R. Hunter, R.L. Weinsier, Electrical impedance in assessing human body composition: the BIA method, Am. J. Clin. Nutr. 47 (5) (1988) 789–792, https://doi.org/10.1093/ajcn/47.5.789.
[17] P. Treleaven, J. Wells, 3D body scanning and healthcare applications, Computer 40 (7) (2007) 28–34, https://doi.org/10.1109/MC.2007.225.
[18] S. Kennedy, P. Hwaung, N. Kelly, Y.E. Liu, S. Sobhiyeh, M. Heo, et al., Optical imaging technology for body size and shape analysis: evaluation of a system designed for personal use, Eur. J. Clin. Nutr. 74 (6) (2020) 920–929, https://doi.org/10.1038/s41430-019-0501-2.
[19] S. Kennedy, B. Smith, S. Sobhiyeh, M.E. Dechenaud, M. Wong, N. Kelly, et al., Digital anthropometric evaluation of young children: comparison to results acquired with conventional anthropometry, Eur. J. Clin. Nutr. 76 (2) (2022) 251–260, https://doi.org/10.1038/s41430-021-00938-x.
[20] S.B. Heymsfield, B. Bourgeois, B.K. Ng, M.J. Sommer, X. Li, J.A. Shepherd, Digital anthropometry: a critical review, Eur. J. Clin. Nutr. 72 (5) (2018) 680–687, https://doi.org/10.1038/s41430-018-0145-7.
[21] L. Rumbo-Rodríguez, M. Sánchez-SanSegundo, R. Ferrer-Cascales, N. García-D'Urso, J.A. Hurtado-Sánchez, A. Zaragoza-Martí, Comparison of body scanner and manual anthropometric measurements of body shape: a systematic review, Int. J. Environ. Res. Public Health. 18 (12) (2021) 6213, https://doi.org/10.3390/ijerph18126213.
[22] G.M. Tinsley, M.L. Moore, J.R. Dellinger, B.T. Adamson, M.L. Benavides, Digital anthropometry via three-dimensional optical scanning: evaluation of four commercially available systems, Eur. J. Clin. Nutr. 74 (7) (2020) 1054–1064, https://doi.org/10.1038/s41430-019-0526-6.
[23] J.P. Bennett, Y.E. Liu, B.K. Quon, N.N. Kelly, M.C. Wong, S.F. Kennedy, et al., Assessment of clinical measures of total and regional body composition from a commercial 3-dimensional optical body scanner, Clin. Nutr. 41 (1) (2022) 211–218, https://doi.org/10.1016/j.clnu.2021.11.031.
[24] B.K. Ng, B.J. Hinton, B. Fan, A.M. Kanaya, J.A. Shepherd, Clinical anthropometrics and body composition from 3D whole-body surface scans, Eur. J. Clin. Nutr. 70 (11) (2016) 1265–1270, https://doi.org/10.1038/ejcn.2016.109.
[25] M.C. Wong, B.K. Ng, S.F. Kennedy, P. Hwaung, E.Y. Liu, N.N. Kelly, et al., Children and adolescents' anthropometrics body composition from 3-D optical surface scans, Obesity (Silver Spring) 27 (11) (2019) 1738–1749, https://doi.org/10.1002/oby.22637.
[26] P.S. Harty, B. Sieglinger, S.B. Heymsfield, J.A. Shepherd, D. Bruner, M.T. Stratton, et al., Novel body fat estimation using machine learning and 3-dimensional optical imaging, Eur. J. Clin. Nutr. 74 (5) (2020) 842–845, https://doi.org/10.1038/s41430-020-0603-x.
[27] S. Sobhiyeh, N. Borel, M. Dechenaud, C.A. Graham, M. Wong, P. Wolenski, et al., Fully automated pipeline for body composition estimation from 3D optical scans using principal component analysis: a Shape UP study, Annu. Int. Conf. IEEE Eng. Med. Biol. Soc. 2020 (2020) 1853–1858, https://doi.org/10.1109/EMBC44109.2020.9175211.
[28] I.Y. Tian, M.C. Wong, S. Kennedy, N.N. Kelly, Y.E. Liu, A.K. Garber, et al., A device-agnostic shape model for automated body composition estimates from 3D optical scans, Med. Phys. 49 (10) (2022) 6395–6409, https://doi.org/10.1002/mp.15843.
[29] M.C. Wong, B.K. Ng, I. Tian, S. Sobhiyeh, I. Pagano, M. Dechenaud, et al., A pose-independent method for accurate and precise body composition from 3D optical scans, Obesity (Silver Spring) 29 (11) (2021) 1835–1847, https://doi.org/10.1002/oby.23256.
[30] I.Y. Tian, B.K. Ng, M.C. Wong, S. Kennedy, P. Hwaung, N. Kelly, et al., Predicting 3D body shape and body composition from conventional 2D photography, Med. Phys. 47 (12) (2020) 6232–6245, https://doi.org/10.1002/mp.14492.
[31] Consultation, W. H. O., "Obesity: preventing and managing the global epidemic." World Health Organization technical report series, 894, 2000, pp. 1–253.
[32] T.N. Hangartner, S. Warner, P. Braillon, L. Jankowski, J. Shepherd, The Official Positions of the International Society for Clinical Densitometry: acquisition of dual-energy X-ray absorptiometry body composition and considerations regarding analysis and repeatability of measures, J. Clin. Densitom. 16 (4) (2013) 520–536, https://doi.org/10.1016/j.jocd.2013.08.007.
[33] B.K. Ng, Y.E. Liu, W. Wang, T.L. Kelly, K.E. Wilson, D.A. Schoeller, et al., Validation of rapid 4-component body composition assessment with the use of dual-energy X-ray absorptiometry and bioelectrical impedance analysis, Am. J. Clin. Nutr. 108 (4) (2018) 708–715, https://doi.org/10.1093/ajcn/nqy158.
[34] M. Loper, N. Mahmood, J. Romero, G. Pons-Moll, M.J. Black, SMPL, a skinned multi-person linear model, ACM Trans. Graph. 34 (6) (2015) 1–16, https://doi.org/10.1145/2816795.2818013.
[35] B.K. Ng, M.J. Sommer, M.C. Wong, I. Pagano, Y. Nie, B. Fan, et al., Detailed 3-dimensional body shape features predict body composition, blood metabolites, and functional strength: the Shape UP! studies, Am. J. Clin. Nutr. 110 (6) (2019) 1316–1326, https://doi.org/10.1093/ajcn/nqz218.
[36] C.C. Glüer, G. Blake, Y. Lu, B.A. Blunt, M. Jergas, H.K. Genant, Accurate assessment of precision errors: how to measure the reproducibility of bone densitometry techniques, Osteoporos. Int. 5 (4) (1995) 262–270, https://doi.org/10.1007/bf01774016.
[37] H. Lee, D. Kim, A. Jung, W. Chae, Ethnicity, social, and clinical risk factors to tooth loss among older adults in the U.S., NHANES 2011–2018, Int. J. Environ. Res. Public Health 19 (4) (2022) 2382, https://doi.org/10.3390/ijerph19042382.
[38] B.H. Duhon, T.T. Phan, S.L. Taylor, R.L. Crescenzi, J.M. Rutkowski, Current mechanistic understandings of lymphedema and lipedema: tales of fluid, fat, and fibrosis, Int. J. Mol. Sci. 23 (12) (2022) 6621, https://doi.org/10.3390/ijms23126621.
[39] A.J. Graybeal, C.F. Brandner, G.M. Tinsley, Visual body composition assessment methods: a 4-compartment model comparison of smartphone-based artificial intelligence for body composition estimation in healthy adults, Clin. Nutr. 41 (11) (2022) 2464–2472, https://doi.org/10.1016/j.clnu.2022.09.014.
[40] A. Nana, J.M.D. Staynor, S. Arlai, A. El-Sallam, N. Dhungel, M.K. Smith, Agreement of anthropometric and body composition measures predicted from 2D smartphone images and body impedance scales with criterion methods, Obes. Res. Clin. Pract. 16 (1) (2022) 37–43, https://doi.org/10.1016/j.orcp.2021.12.006.
[41] G.L. Farina, F. Spataro, A. De Lorenzo, H. Lukaski, A smartphone application for personal assessments of body composition and phenotyping, Sensors (Basel) 16 (12) (2016) 2163, https://doi.org/10.3390/s16122163.
[42] G.M. Tinsley, M.L. Moore, M.L. Benavides, J.R. Dellinger, B.T. Adamson, 3-Dimensional optical scanning for body composition assessment: a 4-component model comparison of four commercially available scanners, Clin. Nutr. 39 (10) (2020) 3160–3167, https://doi.org/10.1016/j.clnu.2020.02.008.
[43] J.A. Shepherd, Y. Lu, A generalized least significant change for individuals measured on different DXA systems, J. Clin. Densitom. 10 (3) (2007) 249–258, https://doi.org/10.1016/j.jocd.2007.05.002.
[44] E. Stark, O. Haffner, E. Kučera, Low-cost method for 3D body measurement based on photogrammetry using smartphone, Electronics 11 (7) (2022) 1048, https://doi.org/10.3390/electronics11071048.
[45] M.D. Majmudar, S. Chandra, K. Yakkala, S. Kennedy, A. Agrawal, M. Sippel, et al., Smartphone camera based assessment of adiposity: a validation study, NPJ Digit. Med. 5 (1) (2022) 79, https://doi.org/10.1038/s41746-022-00628-3.